Glaucoma Screening using Digital Fundus Image through Optic Disc and Cup Segmentation

Megha L. Lotankar
Electronics and Telecommunication Department
St. Francis Institute of Technology
Mumbai, India

Kevin Noronha
Electronics and Telecommunication Department
St. Francis Institute of Technology
Mumbai, India

Jayasudha Koti
Electronics and Telecommunication Department
St. Francis Institute of Technology
Mumbai, India

ABSTRACT
Globally, glaucoma is the major cause of visual impairment. It is a chronic eye disease in which optic nerve damages progressively due to the raised Intraocular Pressure (IOP) of the eye. The technique proposed in this paper allows automatic detection of the glaucoma using digital fundus image by extracting the features like vertical cup to disc ratio (CDR), its area ratio, horizontal to vertical CDR and the ratio of area of blood vessels in inferior-superior region to that in the nasal-temporal region of the Optic Disc (OD) (ISNT Ratio) by segmenting OD, cup and blood vessels. The method proposed for OD segmentation is based on geodesic active contour model. The cup segmentation method is based on the structural properties and color information of the cup region and blood vessels are segmented by morphological technique. The performance evaluation of the proposed technique has been carried out on 200 images comprising 100 normal and 100 glaucomatous images. Support Vector Machine (SVM) is used to classify the fundus images into normal and glaucoma class with sensitivity, specificity, accuracy, Positive Predictive Value (PPV) and Negative Predictive Value (NPV) of 95%, 97%, 96%, 96.94% and 95.10% respectively. The results obtained by proposed technique indicate that the features are clinically important in glaucoma detection.

General Terms
Biomedical image processing, Computer vision, Pattern recognition, Machine learning.

Keywords
Fundus Image, Pallor, Glaucoma.

1. INTRODUCTION
Retinal diseases like cataract, diabetic retinopathy, glaucoma, and macular degeneration are some of the most common causes of vision loss. According to World Health Organization (WHO) glaucoma is the second leading cause of blindness worldwide after cataract. It has been reported that almost 45 million people worldwide have glaucoma and about 79 million people are likely to be suffering from glaucoma by the year 2020 [1]. Glaucoma is a disease in which damage to the optic nerve leads to progressive and irreversible vision loss. Eye pressure (called IOP) is a major risk factor for optic nerve damage. In the early stage of the glaucoma patient don't have any signs of vision loss. But as the glaucoma progresses, patient will encounter the loss of peripheral vision and results into the tunnel vision. The glaucoma is called "silent thief of sight" because vision loss occurs slowly over a long period of time, and symptoms of the diseases occur when the disease is in the advanced stage. Since the optic nerve damage is irremediable, glaucoma can't be cured but early detection and then appropriate treatment can prevent the complete loss of vision. Glaucoma can be detected by three methods: assessment of abnormal vision field, assessment of optic nerve damage and assessment of IOP, out of which the glaucoma assessment by observing optic nerve damage is superior to other two methods [2]. The optic nerve damage can be detected by trained ophthalmologist or through 3D imaging techniques such as Optical Coherence Tomography (OCT) and Heidelberg Retina Tomography (HRT). But optic nerve assessment by specialist is subjective and the equipment cost of OCT and HRT is also high. In this scenario, digital Color Fundus Image (CFI) is a more cost effective imaging technique to assess the damage of the optic nerve; hence in recent years it has been extensively used to diagnosis glaucoma and other ocular diseases. Digital CFI is the image of the fundus taken by a fundus camera or ophthalmoscope. It includes three major structures OD, macula and blood vessels. The OD is a bright yellowish region in the image where ganglion cell axons exit the eye to form the optic nerve, which carries image information of the photo-receptors to the brain. There is no any standard value for OD size; different authors have made different estimations about the size of OD. Li *et al*. [3] have stated that it occupies about one-fifth to one-eighth of the entire fundus image, on the other hand Sinthanayothin *et al.* [4] have pointed out that it occupies about one-seventh of the fundus image. The OD consists of two different regions, a central bright region called the cup and a peripheral region called the neuroretinal rim [5]. Fig. 1 shows different landmarks of CFI. In case of a healthy OD, the size of the cup is very small because it contains more than 1.2 million fibers passing through it, but due to the glaucoma, OD loses its optic nerve fibers which results in increasing the cup size. This enlargement of the cup is an important sign of glaucoma progression [5], hence the vertical CDR and their area ratio are two most important and widely used features of glaucoma detection. But sometimes, people having small CDR have significant loss of vision whereas people having large CDR don't have vision loss [6]. Hence to describe the amount of damage caused by glaucoma

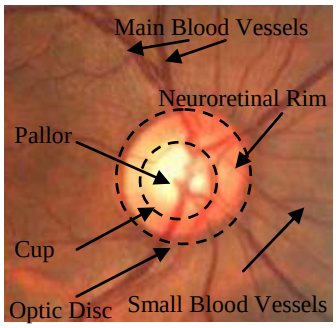

Fig 1: CFI showing landmarks like OD, Cup and Blood Vessels

more precisely, some other features like Peripapillary Atrophy (PPA)[7],Disc Damage Likelihood Scale (DDLS)[6], ISNT ratio[8], disc haemorrhage, neuroretinal rim notching, and Retinal Nerve Fiber Layer (RNFL) defect have been introduced. This paper focus on the four features, vertical CDR, its area ratio, horizontal to vertical CDR and ISNT ratio by segmenting OD and cup. The organization of paper is as follows. Section II contains previous work related to OD and cup detection. Section III gives detailed description of proposed method. Section IV shows the experimental results and section V ends with a conclusion.

2. STATE OF THE ART

Application of image processing and computer vision techniques in ophthalmology has made great progresses in developing automated diagnostic systems for a number of ocular diseases including glaucoma. These techniques are used to detect various fundus features like OD, cup and blood vessels, macula, fovea. Detailed discussion on some earlier published work on OD and cup detection is given in this section.

2.1 Optic Disc Detection

Detection of the OD is a fundamental task for automatic diagnosis of various ophthalmic pathologies like glaucoma, diabetic retinopathy and pathological myopia. Hence, there is a huge literature available on localization and segmentation of the OD. The OD localization finds an OD pixel and the OD segmentation estimate the OD boundary.OD localization methods are proposed in [4] [9] [10] [11]. Sinthanayothin *et al.* [4] has presented a location method in which first fundus images of the intensity channel of the HSI color space were pre-processed by applying an adaptive local contrast enhancement then the OD center was located using the variance of intensity of the adjacent pixels within the OD. Aquino *et al.* [9] used three independent detection methods: Maximum variance method, Maximum difference method , Low pass filter method. OD candidate pixels of each method is obtained and based on these three candidate pixels, the final ODP is decided. Hoover *et al.* [10] located the OD center by determining convergence point of all vessels by fuzzy convergence method. Ying *et al.* [11] has used fractal analysis to discriminate OD from other bright regions like artifacts and exudates in the fundus image, Since all major blood vessels converges at the OD, it has much higher fractal dimension than other brighter regions.OD boundary estimation is categorized into two types namely template matching methods and deformable model based methods. Template matching methods of OD segmentation are proposed in [12] [13] [9]. Lalonde *et al.* [12] has located the OD using pyramidal decomposition. Then canny edge detector is employed to detect the edge map; this edge map is matched with a circular template, using hausdorff distance. Pallawala *et al.* [13] has used Daubechies wavelet transform to localize OD. Then an abstract representation of the OD is used as a template to obtain OD boundary through ellipse fitting algorithm. All these shape-based template matching methods often suffer from restrictions of shape. Aquino *et al.* [9] used the Prewitt edge detector and Circular Hough Transform (CHT) to extract the OD boundary. Next Category of OD segmentation is based on deformable models, proposed in [14] [5] [2]. Li *et al.* [14] has segmented the OD using a modified Active Shape Model (ASM).This method is robust for images with clear OD, but may not work well for low quality images. Joshi *et al.* [5] modified the Chan-Vese active contour model by including regional information in a defined domain. All these methods are usually sensitive to initialization. To overcome the limitations of deformable model based methods, Cheng *et al.* [2] has proposed a superpixel classification based method in combination with the deformable model based methods. Here superpixel classification is used for an initialization of OD boundary and the deformable model is used to get exact OD boundary.

2.2 Optic Cup Detection

Since cup boundary is less visible as compared to OD boundary, in the literature there are very few methods for cup segmentation and results of the existing methods are also preliminary. Nayak *et al.* [8] has segmented the cup region from green channel of RGB color image by morphological operations. Wang *et al.* [15] proposed a cup detection method which is similar to their respective OD segmentation methods. They used a variational level set method in the green channel initialized by p-tile thresholding to detect the optic cup boundary. Joshi *et al.* [16] proposed a cup segmentation method based on the pallor appearance in the OD and the symmetry of cup region. Wong *et al.* [17] proposed one more cup detection method. It is based on bends in blood vessels. Vessels are identified by combination of wavelet transform and edge detection. These vessel edges are evaluated for angular change to obtain the vessel kinks. Joshi *et al.* [5] has also proposed a cup detection method based on blood vessel kinks. They used multi-stage approach to detect the vessel bends and cup boundary is acquired by local spline fitting.

3. METHODOLOGY

An automatic diagnosis system for glaucoma using four features namely vertical CDR its area ratio, horizontal to vertical CDR and ISNT ratio is presented in this paper. The block diagram of the proposed system is shown in Fig. 2.

3.1 Pre-processing

Acquired fundus images are of very high resolution of 2588×1958 pixels. To process these images directly takes a lot of processing time. Hence in order to reduce this processing time, fundus images are resized to 518 x 392 pixels. These fundus images are normally photographed in non-uniform lighting environments. To remove this non-uniformity, Adaptive Histogram Equalization (AHE) technique is used [18]. AHE works on small part of the image, instead of the entire image and computes various histograms, corresponding to a different region of the image. These histograms are used to redistribute the lightness values of the image in order to increases the dynamic range and contrast of an image.

3.2 Feature Extraction

This section includes extraction of features from fundus image.

3.2.1 Cup to Disc Ratio

In 1967, Armaly [19] has developed the concept of CDR. Basically CDR is the ratio of cup diameter to disc diameter. In case of normal eye CDR ranges from 0.2 to 0.5[20] but in

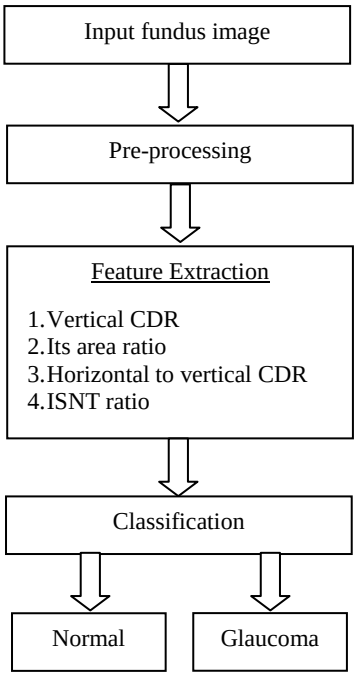

Fig 2: Flow Chart of proposed system

case of the glaucoma, It may reaches up to 1[21]. Vertical CDR is the better measure of deviation than the horizontal CDR, because early neuroretinal rim loss occurs preferentially at the upper and lower poll of the disc. Because vertically oval optic disc and horizontally oval optic cup, the CDR in normal eye is significantly larger horizontally than vertically so the quotient of the horizontal to vertical CDR is usually higher than 1.0[20]. But in case of glaucoma vertical CDR increases faster than the horizontal one so it leads the quotient of the horizontal to vertical CDR to lower than 1.0. Along with vertical and horizontal CDR, their area ratio is also important disk parameters of interest, because vertical or horizontal CDR gives segmentation accuracy only in vertical or horizontal direction but the area ratio gives segmentation accuracy in all direction. For finding the CDR from retinal fundus photographs, the OD and cup must first be extracted.

3.2.1.1 OD Detection

OD detection involves first localization and then segmentation of OD. The developed location methodology obtains Optic Disc Pixel (ODP) by performing frequency domain Gaussian Low-Pass Filtering (GLPF) in the green plane of the RGB color image, as this is the one that provides the best contrast in the image. GLPF can be defined as follows [18]:

$$H(u,v) = e^{\left(\frac{-D^2(u,v)}{2D_0^2}\right)} \quad (1)$$

where $D(u, v)$ is the distance between the origin of the frequency plane and the point (u, v), and D_0 is the cutoff frequency with a value of 25. The pixel which has maximum gray level in the GLPF image is selected as final ODP. Result of this location method is illustrated by the four examples as shown in Fig. 3.

For segmentation of the OD, Region of Interest (ROI) is extracted from the original image. This ROI is 200 × 200 pixels cropped color image centered on an ODP obtained by implemented OD location method. By this way, efficiency and robustness in OD segmentation is increased. Usually OD appears as a clear white shape, brighter than the surrounding

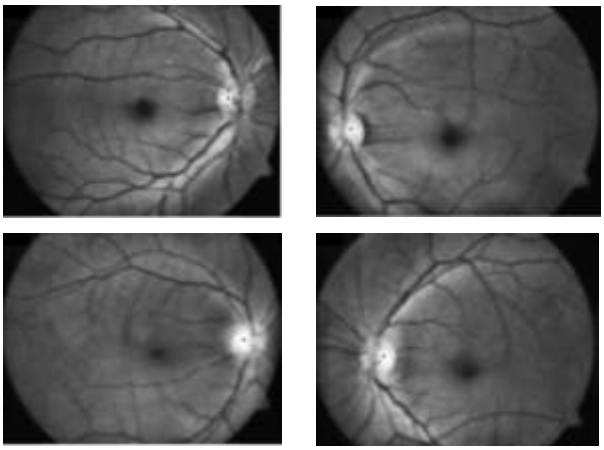

Fig 3: Results of ODP Selection Process

area in the red plane hence red plane is chosen for OD segmentation. The segmentation procedure firstly employs elimination of blood vessels in red plane followed by adaptive thresholding of the resulted red plane to initialize contour by performing CHT [22] to initiate the active contour evolution.Blood vessels elimination procedure involves first detection of blood vessels and then elimination. Blood vessels are detected using bottom-hat filter with linear Structuring Element (SE) of size 20. As there is a great variability in OD appearance, unique threshold establishment is not suitable hence Otsu thresholding method [23] is used to obtain binary image of blood vessels. Because for a gray-level image, it automatically decides a threshold by assuming that it consists of two parts, background and foreground. The method maximizes the between-class variance to set the optimum threshold. After obtaining the blood vessel map, these blood vessels are removed from the OD by using median filter [24]. Firstly a mask image I_m of window size 11×11 pixels is defined for each vessel pixel (i, j), centered at (i, j). Then each vessel pixel's intensity in the red plane image I_r, is replaced by the median of the intensity values of the pixels in its mask image that are not vessel pixels. The obtained image is smoothened by a median filter. Fig. 4 shows the complete process of blood vessels elimination.

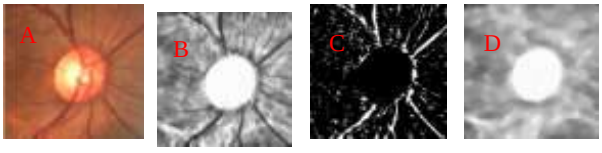

Fig 4: Illustration of the process of Blood Vessels Elimination: (A) ROI, (B) ROI in the Red channel, (C) Binary image of blood vessels, (D) Blood vessels erased image

After elimination of blood vessels, local adaptive thresholding is done on the blood vessel erased image. Local adaptive thresholding selects an individual threshold for each pixel based on the range of intensity values in its local neighborhood to separate desirable foreground image objects from the background. This offers exact initialization of the contour. A good initialization of contour can reduce the computing time and prevent the problem of local maxima/minima. Since the OD can be approximated by a circle in CFI, CHT is used in thresholded images to detect a circle for the range of expected OD radius. CHT can be defined as

$$(a,b,r) = CHT(I_{th}, r_{\min}, r_{\max}) \quad (2)$$

where I_{th} is the thresholded image. $r_{\min}$ and $r_{\max}$ are the minimum and maximum radius limits for the OD. After obtaining the optimal circle for contour initialization, an edge based OD segmentation method known as Geodesic active contour [24] is used. This geodesic active contour connects energy minimization based classical "snakes" and curve evolution theory based geometric active contours [25]. For perfect separation of foreground and background, in this kind of model, these foreground and background are designed statistically and energy function is minimized. Since this model can handle the change in the geometry of the contour, it overcomes some of the drawbacks of the classical active contour model. This contour evolution always converges to the OD boundary by discriminating between OD and Atrophy region but the method is greatly depends on the contour initialization. Fig. 5 shows results of OD segmentation.

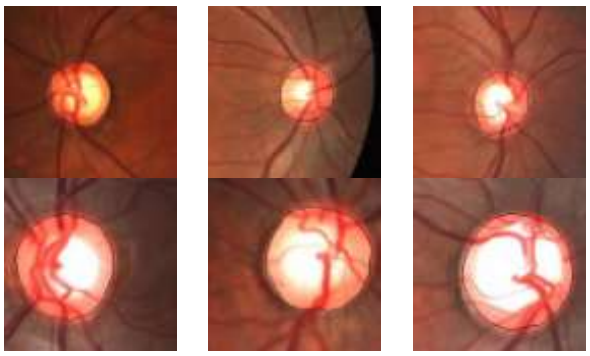

Fig 5: Obtained OD Segmentation on few CFI samples

3.2.1.2 Cup Detection

The fundus images are 2D images so they don't have depth information about the cup region. It increases the difficulty of accurate cup detection hence the ophthalmologists use two main visual clues to obtain the cup boundary from CFI first is the change in color near pallor edge and second is the bending of the small blood vessels [16]. The proposed cup segmentation method is based on appearance of the pallor in the OD region. Since cup region appears well discriminated against the background in the *'a'* plane of *Lab* color space, 'a' plane is chosen for segmentation. Then the binary image of the OD is used as a mask on the 'a' plane of image and '*a'* color plane within OD is used, for further processing, since it reduce the computation. Then a morphological opening with a small circular SE, 'disk' of radius 5 is carried out to smoothened small blood vessels present in the OD. Then the pixels which corresponds to the pallor region are extracted using t= 0.55 threshold. Fig. 6(A) shows 'a' color plane,(B) shows 'a' plane within OD, (C) shows thresholded result superimposed on the original image. This thresholded image covers only the half part of the cup i.e. the temporal region because the nasal side of cup is mostly occluded with the blood vessels. Hence this occluded part i. e. nasal region is obtained by reflecting the temporal side of cup by considering vertical line passing through the OD center as the axis of symmetry as shown in Fig. 6 (D). Then canny edge detector is applied on the resulting image to obtain the cup edges. To get only the cup boundary points a convex hull is applied on the edge detector output (as shown in Fig. 6 (E)). The convex hull is the smallest convex polygon containing all the points. The vertices of the convex hull represent the cup boundary points. These points are connected using cubic spline interpolation technique to get accurate cup boundary (as shown in Fig. 6 (F)).

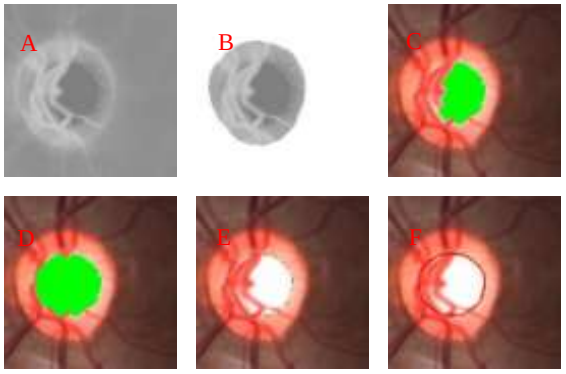

Fig 6: Illustration of the process of cup segmentation: (A) 'a' color plane, (B) 'a' color plane within OD, (C) Thresholded result overlaid on the original image, (D) Reflection of temporal region, (E) Cup boundary points obtained by convex hull, (F) Accurate cup boundary obtained by cubic spline interpolation

The results of the cup detection process are shown in Fig. 7

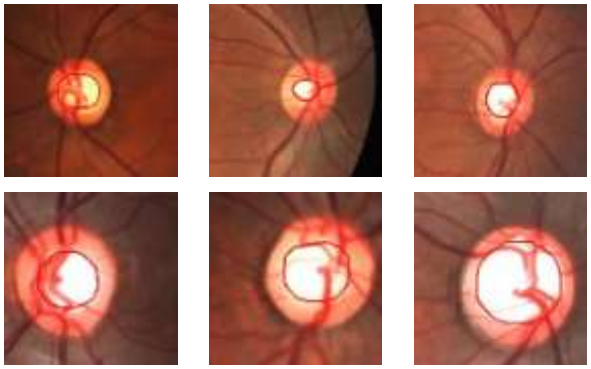

Fig 7: Obtained cup Segmentation on few CFI samples

3.2.2 ISNT Ratio

ISNT ratio is the ratio of area of blood vessels in inferior superior region to that nasal temporal region of OD. Generally the blood vessels are concentrated in the superior and the inferior regions of the OD but in case of glaucoma, blood vessels shifts to nasal side and thus the ISNT ratio will be less compared to normal person. For detecting the blood vessels within OD, first binary image of the OD is obtained by the OD segmentation method described above and used as a mask on the green plane of RGB color image (as shown in Fig. 8 (A)), since blood vessels are brightest in the green plane. The resultant image consists of only the green plane area within OD (as shown in Fig. 8 (B)). Then bottom-hat filtering with

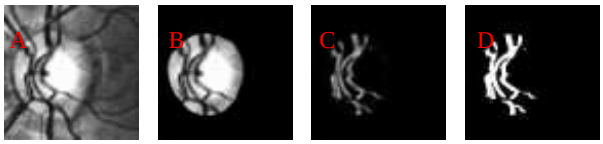

Fig 8: Illustration of blood vessels detection process: (A) Green channel sub-image, (B) Green channel within OD (C) Image after bottom-hat transforms. (D) Binary image of blood vessels

SE of size 20 is applied to highlights the blood vessels within the OD (as shown in Fig. 8 (C)). The binary image of blood vessels is then obtained by Otsu thresholding [22] (as shown in Fig. 8 (D)).The resultant image is cropped to an image of size 150×150 by considering OD center as its center to get only the ROI to reduce the processing time. Then masks of four quadrants are created for extracting blood vessels in each

quadrant. First the mask of one quadrant is obtained and then it is rotated by 90° each time to get remaining three quadrants masks. These masks are used on the ROI to obtain the area of blood vessels in each quadrant. In Fig. 9 top row show the masks used for identifying blood vessels in ISNT quadrants of the OD and bottom row shows the blood vessels in the ISNT quadrants.

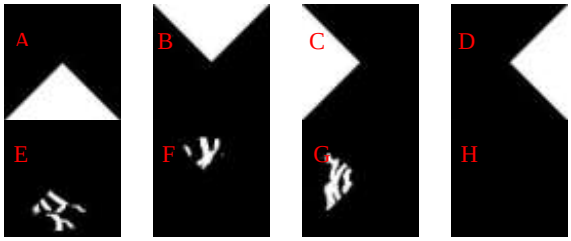

Fig 9: Illustration of the process of ISNT ratio calculation: Top row shows masks used for blood vessels detection in (A) Inferior, (B) Superior, (C) Nasal, and (D) Temporal region and bottom row shows blood vessels in the (E) Inferior, (F) Superior, (G) Nasal, (H) Temporal region

3.3 Classification

Fundus images are classified into normal and glaucoma class using SVM. In machine learning SVMs are supervised learning models used for classification. SVM algorithm is based on the statistical learning theory. SVM uses a linear hyper plane to separate the data set optimally in a higher dimensional plane when the data is non-linearly related to the input plane. When the data is linearly inseparable, a kernel transformation is used to project the data into a new space and then the optimization is carried out in the kernel space. Kernel transformation gives the inner product between two points in a suitable high dimensional space with a small computational cost [26]. The Radial Basis Function (RBF) kernel is used for the classification. There are two parameters for an RBF kernel C and γ. For finding the best values of C and γ, C is varied from 2^{-5} to 2^{5} and γ is varied from 2^{-15} to 2^{3} and 3 fold cross-validation strategy is used. A ten-fold cross validation strategy is employed to test the classifiers. Whole database is divided into ten equal parts. The process begins with the training of first nine parts of the data and testing using remaining one part. The procedure is repeated nine more times for different sets of training and testing data. The average of all the ten folds gives the actual sensitivity, specificity, accuracy, PPV and NPV.

4. EXPERIMENTAL RESULTS

4.1 Database

Proposed method's performance is evaluated on images collected from the Ophthalmology department of Kasturba Medical College, Manipal, India. The ophthalmologists of the department have certified these photographs. The database contents 200 fundus images of the age group of 24–57 year olds in JPEG format with a resolution of 2588×1958 pixels. The fundus images were acquired from a ZEISS retinal camera FF450 plus which provides fundus images of 3.1 megapixels.

4.2 Results

Features such as vertical CDR, its area ratio, horizontal to vertical CDR and ISNT ratio is figured out for whole database using the proposed method. Various statistical measures like sensitivity, specificity, accuracy, PPV and NPV are evaluated to quantify the performance of the proposed method for SVM classifier using these sets of features. Table 1 shows the classification results of SVM using above features. It shows that for the given database the SVM classifier show the best classification sensitivity of 95%, specificity of 97%, accuracy of 96 %, PPV of 96.96% and NPV of 95.1%.

Table 1. Classification Results

Classifier	No. of Features	Sensitivity (%)	Specificity (%)	Accuracy (%)	PPV (%)	NPV (%)
SVM(RBF)	4	95	97	96	96.96	95.1

A confusion matrix of the proposed system is shown in Table 2. A confusion matrix contains statistics of actual and predicted classifications.

Table 2. Confusion Matrix of SVM after 10 fold cross-validation

Class		Predicted	
		Normal	Glaucoma
Actual	Normal	TN = 95	FP = 3
	Glaucoma	PN = 5	TP = 97

Table 3. shows the mean and standard deviations values of computed features along with its *p*-value. From the table it is concluded that, vertical CDR and its area ratio are more for the glaucoma due to the elevated pressure and ISNT ratio is lower for images having glaucoma due to blood vessels shift. *p*-value obtained by student *t*-test is also less than 0.05, this indicate that the features are statistically significant.

Table 3. Mean and standard deviation values for four features and its p-value

Features	Normal Mean ± SD	Glaucoma Mean ± SD	*p*-value
Vertical CDR	0.4065±0.1080	0.6995±0.1031	<0.0001
Its area ratio	0.3363±0.1379	0.6057±0.1615	<0.0001
Horizontal to vertical CDR	1.7562±0.5651	1.1533±0.2124	<0.0001
ISNT Ratio	1.9817±1.3809	1.4324±1.0516	<0.0018

Fig. 10 shows box plots of the four features used for the classification. These box plots show that the median values of features data are different, hence the features are significant.

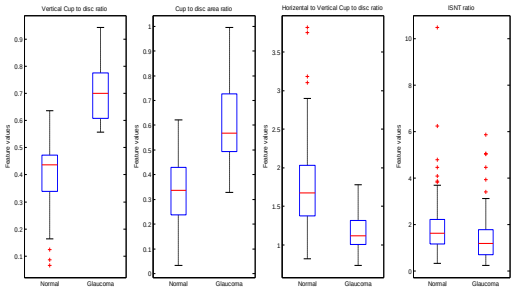

Fig 10: Box plot of vertical CDR, its area ratio, horizontal to Vertical CDR, and ISNT ratio

5. CONCLUSION

In this paper, glaucoma detection method based on the four features vertical CDR, its area ratio, horizontal to vertical CDR and ISNT ratio is presented. The OD from the ROI image is extracted by Geodesic active contours and cup is detected by pallor appearance in the OD and final cup boundary is obtained by spline interpolation technique. Based on the OD and cup segmentation vertical CDR, its area ratio, and horizontal to vertical CDR are calculated. Blood vessels are enhanced using bottom hat filtering and are extracted

using Otsu thresholding technique. Area of blood vessels in each quadrant is obtained by applying mask and ISNT ratio is calculated. Finally SVM classifies the fundus images into Normal and Glaucoma classes based on above extracted features, with sensitivity, specificity, accuracy, PPV and NPV of 95%, 97%, 96%, 96.96 and 95.1% respectively. Obtained results of the proposed method provide an effective solution for glaucoma screening. As a future work one more disc parameter known as DDLS could be a possible direction to improve performance of glaucoma diagnosis.

6. REFERENCES

[1] Pizzarello, et al. VISION 2020: The Right to Sight: a global initiative to eliminate avoidable blindness. Archives of ophthalmology. 2004, 615-620.

[2] Cheng, et al. Superpixel classification based optic disc and optic cup segmentation for glaucoma screening. IEEE Trans. on Medical Imaging. 2013, 1019-1032.

[3] Li, H., and Chutatape, O. Automatic location of optic disc in retinal images. IEEE Intl. Conf. on Image Processing. 2001, 837–840.

[4] Sinthanayothin, C., Boyce, J.F., Cook, H. L. and Williamson, T. H. Automated localization of the optic disc, fovea, and retinal blood vessels from digital color fundus images. British Journal of Ophthalmology. 1999, 902–910.

[5] Joshi, G., Sivaswamy, J. and Krishnadas, S. R. Optic disk and cup segmentation from monocular color retinal images for glaucoma assessment. IEEE Trans. On Medical Imaging. (Jun. 2011), 1192-1205.

[6] Spaeth, G. L., et al. Disc damage likelihood scale: reproducibility of a new method of estimating the amount of optic nerve damage caused by glaucoma. Trans. of American Ophthalmological Society. Soc. 2002, 181–186.

[7] Muramatsu, C., Hatanaka, Y., Sawada, A., Yamamoto, T. and Fujita, H. Computerized detection of Peripapillary chorioretinal atrophy by texture analysis. Engineering in Medicine and Biology Society, EMBC, 2011 Annual Intl. Conf. of the IEEE. 2011, 5947-5950.

[8] Nayak, J., Acharya, R., Bhat, P., Shetty, N. and Lim, T.-C. Automated diagnosis of glaucoma using digital fundus images. Journal of medical systems. 2009, 337–346.

[9] Aquino, A., Gegundez-Arias, M. E. and Marin, D. Detecting the optic disc boundary in digital fundus images using morphological, edge detection, and feature extraction techniques. IEEE Trans. on Medical Imaging. (Nov. 2010), 1860-1869.

[10] Hoover, A. and Goldbaum, M. Locating the optic nerve in a retinal image using the fuzzy convergence of the blood vessels. IEEE Trans. on Medical Imaging. (Aug.2003) 951–958.

[11] Ying, H., Zhang, M., Liu, J.-C. Fractal-based automatic localization and segmentation of optic disc in retinal images. Engineering in Medicine and Biology Society, EMBC 2007. 29th Annual Intl. Conf. of the IEEE. (Aug. 2007), 4139–4141.

[12] Lalonde, M., Beaulieu, M. and Gagnon, L. Fast and robust optic disk detection using pyramidal decomposition and Hausdorff-based template matching," IEEE Trans. on Medical Imaging. (Nov.2001), 1193–1200.

[13] Pallawala, P.M.D.S., Hsu, W., Lee, M. and Eong, K.A. Automated optic disc localization and contour detection using ellipse fitting and wavelet transform. Computer Vision-ECCV, Springer Berlin Heidelberg. 2004, 139-151.

[14] Li, H. and Chutatape, O. Boundary detection of optic disk by a modified ASM method. Pattern Recognition. (Sep. 2003), 2093-2104.

[15] Wong, D.W.K., et al. Level-set based automatic cup-to-disc ratio determination using retinal fundus images in ARGALI. Engineering in Medicine and Biology Society, EMBS 2008. 30th Annual Intl. Conf. of the IEEE. 2008, 2266-2269.

[16] Joshi, G.D., Sivaswamy, J., Karan, K. and Krishnadas, R. Optic disk and cup boundary detection using regional information. IEEE Intl. Symp. On Biomedical Imaging: From Nano to Macro.2010, 948–951.

[17] Wong, D.W.K., Liu, J., Lim, J. H., Li, H. and Wong, T.Y. Automated detection of kinks from blood vessels for optic cup segmentation in retinal images. SPIE, Medical Imaging. Intl. Society for Optics and Photonics. (Mar. 2009).

[18] Gonzalez, R.C. and Woods, R.E. Digital Image Processing, 2nd ed., Prentice Hall, New Jersey, 2001.

[19] Armaly, M. Genetic determination of cup/disc ratio of the optic nerve. Archives of ophthalmology.1967, 35-43.

[20] Bhartiya, Shibal, Gadia, R, Sethi, H. S., and Panda, A. Clinical Evaluation of Optic Nerve Head in Glaucoma. Journal of Current Glaucoma Practice.2010, 115-132.

[21] Noronha, K. P., Acharya, R. U., Nayak, P. K., Martis, R. J. and Bhandary, S. V. Automated classification of glaucoma stages using higher order cumulant features. Biomedical Signal Processing and Control. (Mar. 2014) 174-183.

[22] Duda, R. O. and Hart, P. E. Use of the hough transformation to detect lines and curves in pictures. Communications of the ACM.1972, 11–15.

[23] Otsu, N. A threshold selection method from gray-scale histogram. IEEE Trans. on Syst., Man. Cybern.1978, 62–66.

[24] Yin, F., et al. Model-based optic nerve head segmentation on retinal fundus images. Engineering in Medicine and Biology Society, EMBC 2011. Annual Intl. Conf. of the IEEE. 2011, 2626-2629.

[25] Caselles, V., Kimmel, R., and Sapiro, G. Geodesic active contours. Intl. journal of computer vision. 1997, 61-79.

[26] Vapnik, V. The Nature of Statistical Learning Theory, Springer-Verlag, New York. 1995.